

## InGaAs/InP DHBTs in a planarized, etch-back technology for base contacts

Vibhor Jain<sup>1\*</sup>, E. Lobisser<sup>1</sup>, A. Baraskar<sup>1</sup>, B. J. Thibeault<sup>1</sup>, M. J. W. Rodwell<sup>1</sup>,  
D. Loubychev<sup>2</sup>, A. Snyder<sup>2</sup>, Y. Wu<sup>2</sup>, J. M. Fastenau<sup>2</sup>, W.K. Liu<sup>2</sup>

<sup>1</sup>*Department of Electrical and Computer Engineering, University of California,  
Santa Barbara, CA, 93106-9560, USA*

<sup>2</sup>*IQE Inc., 119 Technology Drive, Bethlehem, PA 18015, USA*

High performance InP DHBTs are required for developing high speed digital logic and mixed signal circuits which will enable sub-mm wave ICs for imaging, sensing, radio astronomy and spectroscopy applications [1]. Lithographic and epitaxial scaling of key DHBT dimensions to reduce transit and RC charging delays is critical for improved transistor bandwidth. Transit delays can be decreased by reducing the base ( $T_b$ ) and collector ( $T_c$ ) thicknesses. However, typical base contact metals - Pd, Ti or Pt diffuse into the base under thermal stress [2], increasing contact resistivity ( $\rho_c$ ) and thus limiting minimum  $T_b$  [3-4]. Hence further base scaling requires non-diffusive metal contacts - W, Mo or Ir which form low  $\rho_c$  contacts to highly doped p-InGaAs [5-6]. These metals are blanket deposited by e-beam evaporation and require planarization and etch-back process to prevent any emitter-base short. In this work, for the first time, we have fabricated InP DHBTs using Pd/W base contact metals in a planarized, etch-back process having simultaneous  $f_\tau/f_{\max} \sim 410/690$  GHz at 220nm wide emitter junction.

For the DHBTs reported here, the InP emitter, InGaAs base and InP collector are 30, 30 and 100 nm thick respectively. Process details for the emitter metal stack and mesa formation are described in [7]. After emitter definition, a thin Pd layer (1.5nm) is blanket deposited by e-beam evaporation followed by a 20 nm sputtered W deposition to form the base contact. The W deposition is conformal, hence to prevent base-emitter short-circuits, W is etched from the sides of the emitter using a photo-resist planarization and etch-back technique [8]. Ti/Au pads for the base were lifted-off to reduce base metal resistance. Devices are isolated by dry etching Pd and W in the field using a SiN<sub>x</sub> hard mask. Remainder of the process is as in [7].

Emitter access resistance  $\rho_{ex} = 6 \Omega\text{-}\mu\text{m}^2$  was extracted from RF data. HBTs with an emitter area  $A_{je} = 0.22 \times 5.7 \mu\text{m}^2$ , have peak  $\beta = 26$ , with common emitter breakdown voltage  $V_{BR,CEO} = 2.4$  V ( $J_e = 10 \mu\text{A}/\text{cm}^2$ ). Kirk effect is observed at  $J_e = 21 \text{ mA}/\mu\text{m}^2$  where the  $f_\tau$  falls to 95% of its peak value. 1-67 GHz measurements of HBTs were carried out after performing a standard line-reflect-reflect-match (LRRM) calibration on an Agilent E8361A PNA, bringing the reference planes to the probe tips. On wafer, short and open circuit pad structures identical to those used by the devices were measured after calibration to de-embed associated transistor pad parasitics from device measurements. Peak RF performance was obtained at  $I_c = 22.4$  mA and  $V_{ce} = 1.67$  V ( $J_e = 17.9 \text{ mA}/\mu\text{m}^2$ ,  $P = 29.9 \text{ mW}/\mu\text{m}^2$ ). Extrapolations from single pole fit indicate  $f_\tau = 410$  GHz and  $f_{\max} = 690$  GHz.

In this process, we have used Pd/W contacts for achieving low  $\rho_c$ . However, the technique is readily extended to incorporate any low resistivity, refractory base ohmic in a DHBT process flow. This will lead to further improvement in transistor performance.

[1] M. J. W. Rodwell et al., Proceedings of the IEEE 96, pp. 271-286 (2008)

[2] E. F. Chor et al., Journal of Applied Physics, Vol 87, No 5, pp. 2437-2444 (2000)

[3] Z. Griffith et al., IEEE Int. Conf. on Indium Phosphide and Related Materials, pp. 96-99, (2006)

[4] Z. Griffith et al., Compound Semiconductor Integrated Circuit Symposium, CSIC IEEE, pp. 275-278, (2006)

[5] Ashish Baraskar et al., Electronic Materials Conference, South Bend, Indiana, USA, (Jun 2010)

[6] Ashish Baraskar et al., 16<sup>th</sup> Int. Conf. on Molecular Beam Epitaxy, Berlin, Germany (Aug 2010)

[7] Vibhor Jain et al., Electron Device Letters 32, pp. 24-26 (2011)

[8] Greg Burek et al., Journal of Crystal Growth, Volume 311, Issue 7, pp. 1984-1987 (2009)

Portion of this work was done in the UCSB nanofabrication facility, part of the NSF-funded NNIN network.

\*Corresp. author: vibhor@ece.ucsb.edu, Phone: +1-805-893-3273, Fax: +1-805-893-3262

T(nm)	Material	Doping (cm <sup>-3</sup> )	Description
10	In <sub>0.53</sub> Ga <sub>0.47</sub> As	> 5·10 <sup>19</sup> : Si	Emitter Cap
15	InP	5·10 <sup>19</sup> : Si	Emitter
15	InP	2·10 <sup>18</sup> : Si	Emitter
30	InGaAs	9·5·10 <sup>19</sup> : C	Base
4.5	In <sub>0.53</sub> Ga <sub>0.47</sub> As	9·10 <sup>16</sup> : Si	Setback
10.8	In <sub>0.53</sub> Ga <sub>0.47</sub> As / In <sub>0.52</sub> Al <sub>0.48</sub> As	9·10 <sup>16</sup> : Si	B-C Grade
3	InP	6·10 <sup>18</sup> : Si	Pulse doping
81.7	InP	9·10 <sup>16</sup> : Si	Collector
7.5	InP	1·10 <sup>19</sup> : Si	Sub Collector
7.5	In <sub>0.53</sub> Ga <sub>0.47</sub> As	4·10 <sup>19</sup> : Si	Sub Collector
300	InP	2·10 <sup>19</sup> : Si	Sub Collector
-625,000	InP	SI	Substrate

Table 1. DHBT layer structure

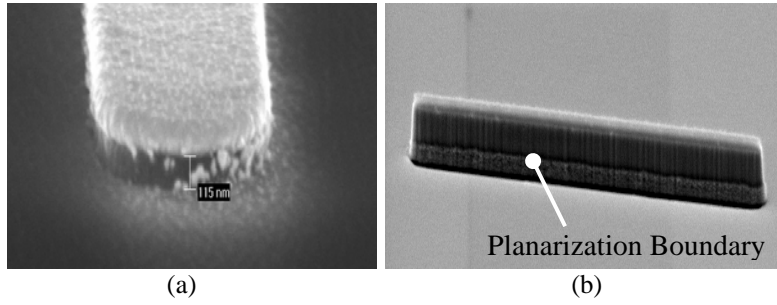


Fig 1. SEMs of the emitter during planarization and etch-back steps (a) Emitter projecting from PR during planarization; (b) Emitter after W etch back showing the planarization boundary

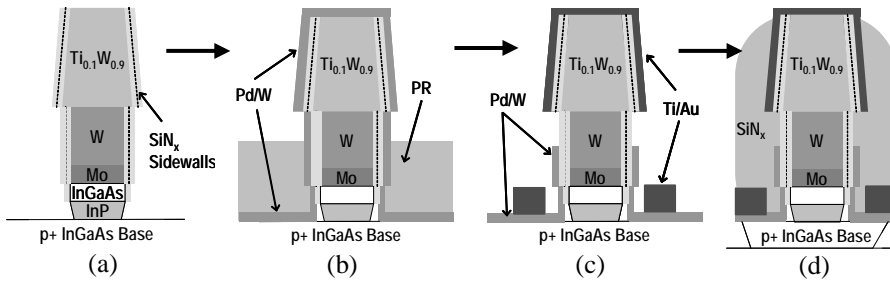


Fig 2. Base process flow - (a) Emitter metal stack and mesa formation; (b) Blanket Pd/W deposition, PR planarization; (c) W etch from the sides of emitter and Ti/Au pad lift-off; (d) Base mesa formed by dry etching Pd/W in the field and wet etch of base semiconductor using SiN<sub>x</sub> hard mask

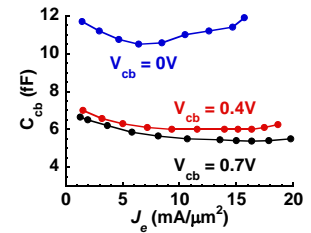


Fig 3. Variation in  $C_{cb}$  with  $V_{cb}$  and  $J_e$ ;  $C_{cb}$  is extracted from  $Y_{12}$  at 5 GHz

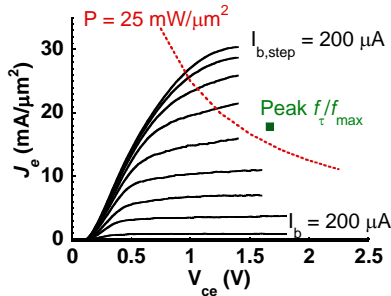


Fig 4. DHBT Common-Emitter  $I$ - $V$  characteristics;  $A_{je} = 0.22 \times 5.7 \mu\text{m}^2$

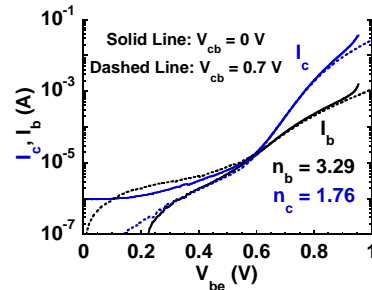


Fig 5. Gummel Plot of DHBT with  $A_{je} = 0.22 \times 5.7 \mu\text{m}^2$

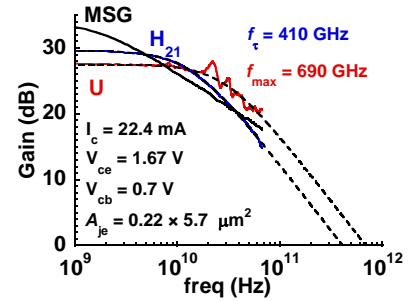


Fig 6. Measured RF gains for the DHBT in 1 - 67 GHz band

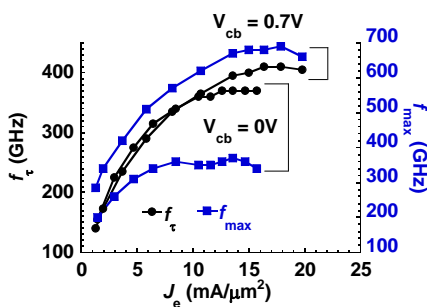


Fig 7.  $f_{\tau}/f_{\text{max}}$  dependence on  $V_{cb}$  and  $J_e$

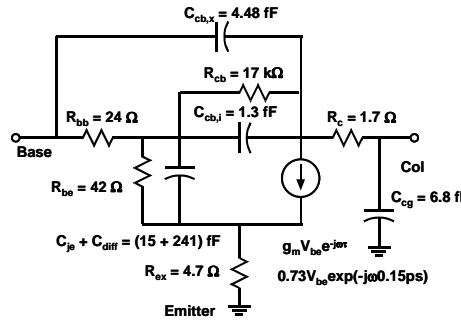


Fig 8. Hybrid- $\pi$  equivalent circuit at peak RF performance derived from 1 - 67 GHz RF data

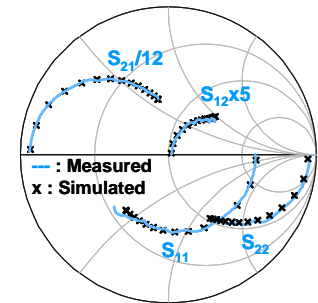


Fig 9. 1 - 67 GHz measured and simulated S-Parameters from equivalent circuit model in Fig 8